Structural and optical properties of GaInNAs/GaAs quantum structures

2004 J. Phys.: Condens. Matter 16 S3009

(http://iopscience.iop.org/0953-8984/16/31/002)

INSTITUTE OF PHYSICS PUBLISHING JOURNAL OF PHYSICS: CONDENSED MATTER

J. Phys.: Condens. Matter **16** (2004) S3009–S3026 PII: S0953-8984(04)75460-0

Structural and optical properties of GaInNAs/GaAs quantum structures

T Hakkarainen[1,2], J Toivonen[1,3], H Koskenvaara[1], M Sopanen[1] and H Lipsanen[1]

[1] Optoelectronics Laboratory, Helsinki University of Technology, PO Box 3500, FIN-02015 HUT, Finland
[2] Optoelectronics Research Centre, PO Box 692, FIN-33101 Tampere, Finland
[3] Laboratory of Biophysics, University of Turku, PO Box 123, FIN-20521 Turku, Finland

E-mail: teppo.hakkarainen@orc.tut.fi

Received 26 January 2004
Published 23 July 2004
Online at stacks.iop.org/JPhysCM/16/S3009
doi:10.1088/0953-8984/16/31/002

Abstract

Structural and optical properties of GaInNAs/GaAs quantum structures grown by metalorganic vapour phase epitaxy (MOVPE) are studied. The growth of arsenide–nitrides by MOVPE is reviewed and compared to the other major growth technique, molecular beam epitaxy. Post-growth thermal annealing and laser irradiation are employed and found to affect GaInNAs quantum wells differently: with laser treatment no undesired blue-shift of the photoluminescence peak is observed. The critical thickness for misfit dislocation formation of GaAsN on GaAs is found to be about twice as large as the theoretical prediction. GaAsN epilayers are also found to contain Ga vacancies in defect complexes. The current status of experimental research on GaInNAs quantum dot structures is reviewed. Self-organized and strain-induced GaInNAs quantum dots are grown and their formation and optical properties are studied. The emission wavelength of InGaAs quantum dots is extended by using InGaAs and GaInNAs barrier layers.

1. Introduction

Transmitters with long-wavelength semiconductor lasers are key components in the development of optical fibre networks for the internet and data traffic. Today's high-speed lasers operating at 1.3 and 1.55 μm wavelengths are made of InP-based heterostructures. However, the GaInAsP/InP laser structures have some shortcomings such as low characteristic temperature and inapplicability to vertical-cavity surface-emitting lasers (VCSELs). Low characteristic temperature coefficient is due to the existence of small band gap discontinuities between the conduction bands of InP and GaInAsP and cannot be significantly improved by band gap engineering. Due to the small refractive index difference of InP-based materials, it

is very difficult to realize the distributed Bragg reflector mirrors needed for a VCSEL. More cost-effective GaAs-based VCSELs are used in short-range optical communication at 850 nm wavelength. Therefore, for several years there has been a lot of activity in developing GaAs-based active material for long-wavelength lasers.

GaInNAs was proposed by Kondow *et al* [1] as a material that could be grown lattice matched on GaAs with the possibility of reaching light emission at 1.3 μm and beyond due to the large band gap bowing with increasing nitrogen composition. The study of GaInNAs and other III–V–N semiconductors has been increasing ever since. Besides its cost-effectiveness and robustness, GaInNAs can be used to prepare monolithic VCSELs [2–4], which would be ideally suited for 1.3 μm transmission systems. Moreover, GaInNAs edge-emitting lasers [5–8] could be used in Raman amplifiers in wavelength division multiplexing architectures. Raman amplification requires output powers close to 1 W in single mode. Such power levels seem to be out of the reach of GaInAsP/InP or AlGaInAs/InP lasers. Recently, GaInNAs has also been employed to fabricate semiconductor saturable absorber mirrors used for mode-locking in a fibre laser system operating at 1.5 μm [9].

Although promising device results have been obtained, the material properties of GaInNAs are still not completely understood. GaInNAs exhibits interesting new properties and differs considerably from the conventional III–V alloys, such as InGaAs, AlGaAs and GaInAsP. Significant changes occur in the electronic band structure compared to GaAs with incorporation of only a small fraction of nitrogen into GaAs. These include a large red-shift of the band gap [10–15], an increase in the electron effective mass [16–18], a highly nonlinear pressure dependence of the band gap [19, 20] and the N-induced formation of new bands [14, 15, 20, 21]. A number of theoretical approaches such as a band anti-crossing model [20, 22, 23], an empirical pseudopotential method [24–27] and $\mathbf{k} \cdot \mathbf{p}$ models [28, 29] have been proposed to describe all the above mentioned phenomena. However, modelling the properties of GaInNAs has been found to be difficult and the models often yield conflicting results. Review articles have been written on the material properties and lasing features of dilute nitride semiconductors [30–33]. Therefore, we choose not to repeat the basic material features of GaInNAs in this paper. Instead, we focus on our studies on the structural and optical properties of GaInNAs/GaAs quantum well (QW) and quantum dot (QD) structures and GaAsN epilayers grown by MOVPE.

2. Experiments

MOVPE growth was carried out on GaAs(100) substrates in a horizontal atmospheric pressure reactor having a cross-sectional area of 3 cm^2. Trimethylgallium (TMGa), trimethylindium (TMIn), tertiarybutylarsine (TBAs), tertiarybutylphosphine (TBP) and dimethylhydrazine (DMHy) were used as sources for gallium, indium, arsenic, phosphorus and nitrogen, respectively. Typical growth temperatures for GaInNAs material were in the range 500–550 °C. All the temperatures mentioned here are thermocouple readings. *In situ* and post-growth annealing was performed under excess As ambient in the MOVPE reactor to improve the optical quality of the materials. The structural properties were studied using several techniques. The surface morphology of the material was investigated by means of a contact-mode atomic force microscope (AFM) using SiN tips. High-resolution x-ray diffraction (HRXRD) was used to determine the thickness and the composition of the grown epitaxial layers. Misfit dislocations in the epilayers were detected by synchrotron x-ray topography measurements performed at the HASYLAB-DESY, Hamburg, Germany. Positron annihilation spectroscopy in Doppler-broadening mode was used to study vacancies in the MOVPE-grown GaAsN. The optical properties of the samples were characterized by photoluminescence (PL) spectroscopy and time-resolved PL measurements.

3. Growth of GaInNAs

Dilute nitrides like GaAsN and GaInNAs differ from many other III–V semiconductors because their binary constituents have sub-lattices with different crystal structures, and there is an alloy miscibility gap [34]. Experiments indicate that GaInNAs should be grown at a reduced growth temperature under highly non-equilibrium nucleation conditions. If either the growth temperature or the mole fraction of nitrogen is too high, phase segregation occurs and the alloy breaks up into microscopic regions of GaInN and GaInAs, resulting in very poor optical properties [31]. This section gives a short review of some of the important issues related to the MOVPE growth of dilute nitrides and contrasts these to the other major epitaxial growth technique, molecular beam epitaxy (MBE).

GaInNAs is a relatively new material, and the most suitable combination of precursors for MOVPE growth is not yet clear. A low growth temperature of 500–600 °C is needed for N incorporation. Therefore, precursors should have low decomposition temperatures. It is also important to choose precursors which are known to generate low background impurity concentrations. The gallium precursor used in this work, TMGa, decomposes incompletely at low temperatures. Thus, the growth rate decreases when the temperature is decreased. We measured the decrease in the growth rate to be 10% at 540 °C and 15% at 520 °C compared to the growth rate at temperatures above 600 °C. The other commonly used gallium source, triethylgallium (TEGa), has a lower decomposition temperature and provides a constant growth rate at temperatures from 700 °C down to 500 °C [35]. Unintentional carbon doping is greatly enhanced at low growth temperatures when using TMGa [36]. This is due to a stable monomethylgallium molecule and is avoided by using TEGa. Overall, TEGa is considered a more suitable source of Ga for low-temperature-grown arsenide–nitrides than TMGa [37]. The most common source for arsenic in MOVPE is gaseous and very toxic arsine. TBAs is a less hazardous arsenic source and also has about 200 °C lower decomposition temperature than arsine [38]. Several precursors have been used to incorporate nitrogen in arsenide–nitrides. Nowadays the most widely used N source for the MOVPE of arsenide–nitrides is DMHy, even though very low N incorporation efficiency is observed. Indeed, we found that in the growth of GaAsN with DMHy the distribution coefficient of nitrogen over arsenic is very low, 0.0052. However, we were still able to achieve a composition of $0 < x < 0.056$ for $GaAs_{1-x}N_x$ with DMHy [39]. Other nitrogen sources used for MOVPE and metalorganic MBE, hydrazine [35], monomethylhydrazine [40], tertiarybutylhydrazine [41, 42] and nitrogen trifluoride (NF_3) [35], have been reported to incorporate nitrogen more efficiently than DMHy. A common feature of hydrazine-type precursors is that they all release NH_2 radicals when they decompose. The large number of different radicals in the gas phase leads to very complicated reactions and the properties of the grown crystal may vary greatly between different types of reactor.

Figure 1 shows the effect of the growth temperature on the N composition of $Ga_{1-y}In_yN_xAs_{1-x}$ QWs. Two In compositions of $y = 0.1$ and 0.3 were used. Typically for MOVPE growth, the N composition decreases rapidly with increasing growth temperature. This effect is even more pronounced with a larger In concentration and is probably caused by the enhanced N desorption from the surface [43]. The optimum growth temperature for N incorporation in our reactor was found to be 520 °C. Decreasing the growth temperature below this limit resulted in poor crystal quality. Drawbacks of the low growth temperature are the increased impurity concentrations [36, 44] and the deteriorated material properties of arsenide–nitrides [45, 46]. Thus, the determination of the growth temperature is a compromise between the N incorporation efficiency and the material quality. Figure 1 also shows the well-known inverse dependence of the N incorporation on the In concentration [47–49]. Due to this effect, one needs to use very high DMHy/V ratios of above 0.9 to incorporate a few per cent

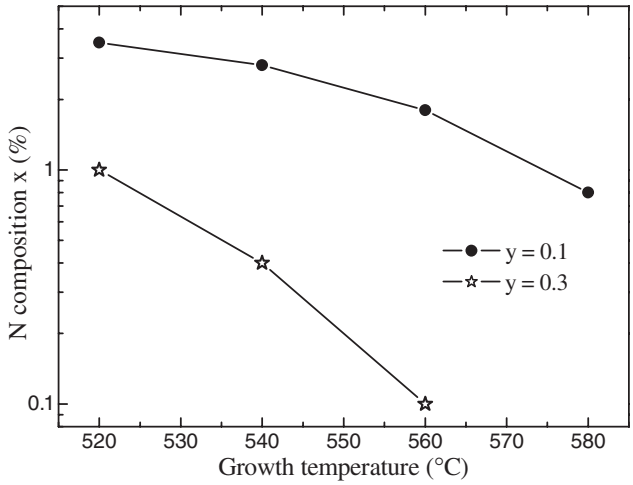

Figure 1. Nitrogen composition x of $Ga_{1-y}In_yN_xAs_{1-x}$ as a function of growth temperature for In compositions $y = 0.1$ and 0.3.

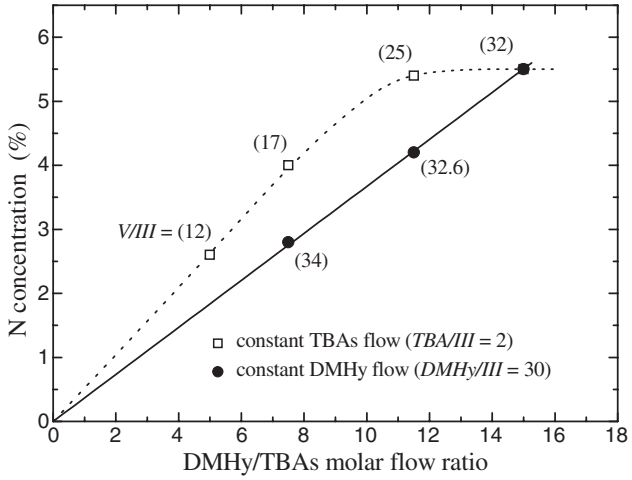

Figure 2. Effect of DMHy/TBAs molar flow ratio on the N concentration of GaAsN/GaAs MQW structures. The V/III ratio of each sample is shown in parentheses and the lines are guides to the eye.

of nitrogen into strained GaInNAs QWs [49]. The cause of this effect is still not completely clear, but it is directly related to the chemistry of DMHy, TMGa and TMIn precursors. TMGa and TMIn produce reactive CH_3 radicals, which might affect the N incorporation by forming methylamine with NH_2 radicals [35, 41]. In contrast to the hydrazine-type nitrogen sources, layers grown with NF_3 show only a minimal dependence of the nitrogen content on the In concentration [41].

Figure 2 shows the effect of the DMHy/TBAs ratio on the N concentration of the GaAsN layers grown at 530 °C. At such a low growth temperature a low TBAs/III ratio of about two is sufficient for the surface protection of GaAsN. When the TBAs flux is kept constant (TBAs/III = 2), the N concentration increases linearly with increasing DMHy flux up to 5% and then saturates to 5.6%. The dependence of the N concentration on the TBAs flux is also linear, the N concentration increases with decreasing TBAs/III ratio. However, when the

TBAs/III ratio was decreased below 2, no high-quality crystal growth was observed because the surface protection was lost. The N concentration becomes more and more sensitive to the V/III ratio with increasing DMHy/V ratio. In order to incorporate over 2% of nitrogen into GaAs, more than 80% of the total group-V gas flow has to be DMHy.

MBE differs in many ways from MOVPE in the growth of arsenide–nitrides, especially when elemental solid sources are used. Pure reactive atomic sources are delivered to the MBE chamber and the growth is performed in vacuum. In such conditions, much lower growth temperatures can be used. The decomposition of precursors and the prereactions between them are not a concern. Nitrogen is produced from a radio-frequency plasma source, which allows for growth at low temperature. However, there are also several kinds of nitrogen ion in plasma, like N^+ and N^{2+}, that can form severe defects when tunnelling into the growing structure. Opposite to MOVPE, the In and N compositions in MBE can be controlled independently [43, 50]. The sticking probability of nitrogen is reported to be very high; virtually all the incident nitrogen atoms incorporate into the crystal [31, 43] as long as the growth temperature is below 500 °C and the V/III ratio is not too large [51]. Also unlike in MOVPE, resultant N composition in MBE appears to be inversely proportional to the group-III growth rate [51]. Not much is known about the effects of the V/III beam flux ratio on optical properties of MBE-grown GaInNAs. In the studies by Kondow *et al* [52] the emission wavelength exhibited a parabolic behaviour as the V/III ratio was varied. However, the V/III ratio does not seem to have such a drastic effect on the alloy composition or nitrogen sticking probability as in MOVPE.

It is clear that the growth of arsenide–nitrides is a complicated task, regardless of the growth method. The PL intensity of GaInNAs deteriorates very rapidly with increasing N concentration. Perhaps the best strategy for obtaining device-quality $Ga_{1-y}In_yN_xAs_{1-x}$ is to introduce a minimum amount of nitrogen and maintain the QW under maximum compressive strain. The finding that x should be kept as small as possible is further validated by the observations that nitrogen induces large alloy fluctuations in $Ga_{1-y}In_yN_xAs_{1-x}$ [30, 53, 54]. Large x also reduces material gain very significantly. Although the growth of GaInNAs is perhaps more easily controlled in MBE, MOVPE has advantages over MBE in production related issues like easy maintenance, high growth rates, high uptime and lower total expenses. After a careful optimization of growth conditions, the difference in the resulting material quality is typically small between MBE and MOVPE. Indeed, good GaInNAs lasers have been fabricated using both growth methods [55–59].

4. Optical properties of GaInNAs

Arsenide–nitrides show luminescence properties that are typical for materials exhibiting exciton localization at the band edges due to potential fluctuations [60]. The spectral shape of the luminescence changes at different temperatures. The PL peak has an exponential low-energy tail at low temperatures <200 K caused by the emission from the localized states below the conduction band edge. At higher temperatures >300 K the PL peak has a typical high-energy tail caused by the emission from the thermally populated delocalized states of the energy band. The transition from the localized exciton emission to the band edge emission with increasing temperature causes an S-shaped behaviour for the PL peak energy as a function of the temperature [61]. Long PL decay times have been measured for arsenide–nitrides at low temperatures [53, 61]. The PL decay times of over 4 ns have been found for the localized states in the low-energy tail, whereas the high-energy edge of the PL peak exhibits a decay time of less than 500 ps. This short decay time at the high-energy edge is attributed to the diffusion of the delocalized excitons to the rapid non-radiative centres. At room temperature no such behaviour is found.

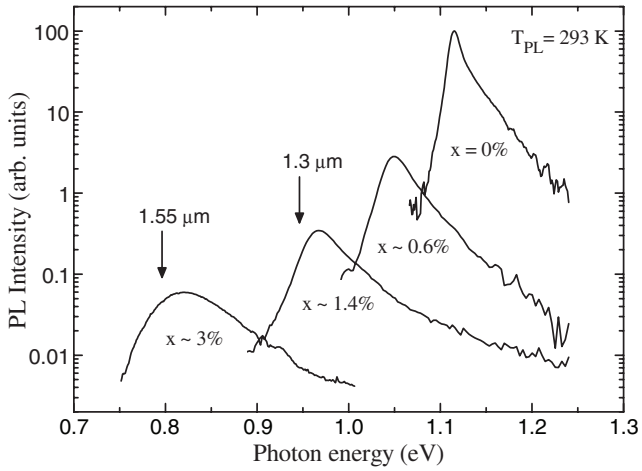

Figure 3. Room-temperature PL spectra of 6 nm-thick $Ga_{0.68}In_{0.32}N_xAs_{1-x}$ QWs with $x = 0$, 0.006 and 0.014. The spectrum of a 9 nm-thick $Ga_{0.74}In_{0.26}N_{0.03}As_{0.97}$ QW is also shown.

As-grown GaInNAs samples exhibit very poor optical activity and, therefore, need to be annealed. Post-growth annealing treatment increases PL intensity usually by a factor of 10–100. This is due to an improvement in the structural quality of the material via annihilation of non-radiative recombination centres [62]. Deep-level transient spectroscopy studies indicate that some carrier traps almost completely disappear on annealing, while others are very persistent [63, 64]. Unfortunately, annealing also causes an undesired blue-shift of the PL emission. Two distinct mechanisms have been proposed for the origin of the blue-shift. One relies on the diffusion of N out of the GaInNAs QW and Ga, In or N interdiffusion at the QW interfaces [65–67]. The second proposed microscopic mechanism causing a blue-shift is associated with local atomic clustering. Because GaInNAs is not a perfectly random alloy, the band gap is not exactly controlled by the compositions x and y. GaInNAs has been shown to contain short-range N-centred N-In_mGa_{4-m} ($0 \leqslant m \leqslant 4$) clusters [25, 68, 69]. According to the local density approximation [70], increasing the number of In–N nearest neighbour bonds from 0 to 4 increases the band gap by as much as 150 meV. This change in m gives rise to five discrete band gaps for a fixed macroscopic composition. Thus, the annealing induced blue-shift would originate from the re-arrangements of these atomic clusters.

We found the optimum annealing condition for PL intensity in our MOVPE reactor to be 10 min at 700 °C [49]. Figure 3 shows room-temperature PL spectra of $Ga_{1-y}In_yN_xAs_{1-x}$ QWs annealed at this optimum condition. The rapid decrease of the PL intensity with increasing N composition can be clearly seen. We were able to reach 1.61 μm low-temperature PL emission from a $Ga_{0.74}In_{0.26}N_{0.03}As_{0.97}$/GaAs multiple QW structure. After annealing, this sample exhibited room-temperature luminescence at 1.51 μm. Experimental findings suggest that x should not exceed 0.02 for device applications. With $x \approx 0.02$ the wavelength of 1.5 μm cannot be reached if a simple GaInNAs/GaAs QW structure is used. However, GaAsN strain-compensating and/or GaInNAs strain-mediating layers grown on both sides of the QW have been used to push the emission wavelength well beyond 1.3 μm [71]. Interestingly the strength of the PL is not much deteriorated when these layers are used. The emission wavelength can also be increased by alloying antimony into GaInNAs [72–77]. Besides shrinking the band gap, Sb acts as a surfactant improving the surface kinetics and thus maintaining two-dimensional growth under high surface stress. It looks like GaInNAsSb would allow for slightly larger In

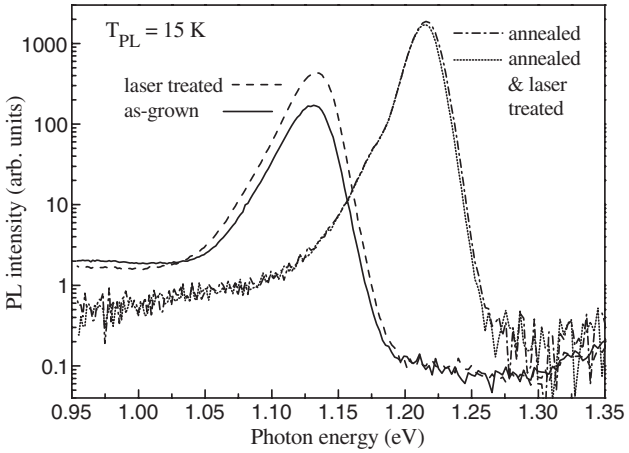

Figure 4. PL spectra measured at 15 K before and after thermal annealing and laser treatment of a $Ga_{0.8}In_{0.2}N_{0.02}As_{0.98}$ QW structure. The PL excitation and the laser treatment intensities were 42 and 10 000 W cm^{-2}, respectively.

composition to be used in the QW without causing phase separation or lattice relaxation via misfit dislocations [72].

In addition to the post-growth annealing, the luminescence intensity can be increased by laser treatment [78]. We have studied the effects of laser irradiation on the optical properties of 5 nm-thick GaInNAs QWs (see [79] for details). The effects of thermal annealing and laser treatment were found to differ from each other. Figure 4 shows PL spectra measured at 15 K from a $Ga_{0.8}In_{0.2}N_{0.02}As_{0.98}$ QW structure before and after both thermal annealing and laser treatment. Thermal annealing causes a 10-fold increase in the PL intensity but shifts the PL peak by 86 meV to higher energies. This behaviour can be explained by the annihilation of non-radiative recombination centres and the local re-arrangements of the In and N atoms as discussed earlier in this section.

Laser treatment on the other hand increases the PL intensity but the blue-shift of the PL peak is negligible. The laser treatment procedure affects the defects most likely due to recombination-enhanced defect reactions [78, 80]. A high density of carriers is generated in the material by the laser beam and the carriers focus their energy on the volumes with the fastest recombination channels. Thus, the changes in atomic configurations are possible only in the vicinity of the fast non-radiative recombination centres. Laser treatment has no impact on the optical properties of a thermally annealed GaInNAs sample. This can be explained as follows: when GaInNAs is annealed the whole lattice gains thermal energy, the local configuration around a nitrogen atom changes [69], and the defect that can be affected by laser treatment disappears. Laser irradiation could offer advantages in the cases like long-wavelength structures, where the blue-shift of the PL peak should be avoided. The effects were observed at laser irradiation intensities encountered sometimes in PL measurement conditions. Therefore, the effects of laser irradiation should be taken into account when measuring the optical properties of GaInNAs samples.

5. Structural properties of GaAsN

5.1. Surface morphology and misfit dislocations

The surface morphology of arsenide–nitrides has been found to change from an atomically flat surface into three-dimensional structures when the N composition is increased [81–83].

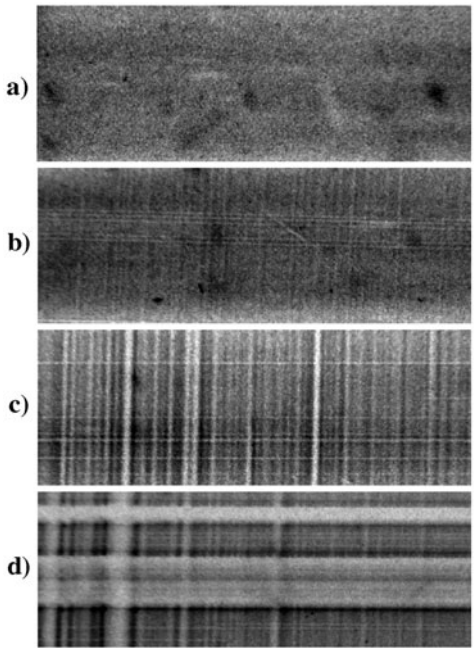

Figure 5. 311 back-reflection synchrotron topographs (620 μm × 220 μm) of as-grown $GaAs_{0.965}N_{0.035}$ layers on GaAs with a thickness of (a) 40 nm, (b) 80 nm, (c) 220 nm and (d) 500 nm. When the critical thickness is exceeded, misfit dislocations seen as white lines appear in the images.

Low growth temperature required for the N incorporation prevents the step-flow growth of the material. The possible reasons for the three-dimensional structures at high N compositions are an insufficient arsenic protection of the surface and the high strain between the substrate and the epilayer. We studied the surface morphology of GaAsN on GaAs with AFM [84]. The roughness of the surface of an as-grown 130 nm-thick $GaAs_{0.965}N_{0.035}$ epilayer was more than one monolayer. Due to annealing at 700 °C the surface was smoothed and the atomic steps were clearly seen. The three-dimensional surface structures were not observed even at N compositions over 4%. We have shown that the $GaAs_{1-x}N_x$ with the N composition x up to 0.056 can be grown without a significant surface degradation as long as the surface protection with arsenic is sufficient [39].

In order to grow high quality strained GaAsN epilayers on GaAs, it is important to know the critical thickness of misfit dislocation formation for the material system. Uesugi *et al* [85, 86] studied the critical thickness of $GaAs_{1-x}N_x$ on GaAs with different N compositions using a HRXRD mapping technique. However, the technique is not sensitive to single misfit dislocations but rather to average relaxation of the strain. This leads easily to the overestimation of the critical thickness. We have studied the strain relaxation mechanism in the strained $GaAs_{1-x}N_x$ on GaAs structures by synchrotron x-ray topography [84]. In epilayers thicker than the critical thickness, an isotropic and a uniform misfit crosshatched dislocation network along two mutually perpendicular ⟨110⟩ directions was observed (figure 5). As the total strain was further increased by increasing the N composition or the epilayer thickness, the dislocations accumulated and the strain relaxation was found to continue through the cracks in the epilayer. However, some areas of the epilayer still remained highly strained. The critical thickness for $GaAs_{1-x}N_x$ on GaAs was determined with the two N compositions of $x = 0.009$ and 0.035. For the 500 nm-thick $GaAs_{1-x}N_x$ epilayer with $x = 0.009$ a very low misfit dislocation density

was found, which indicates that the epilayer thickness slightly exceeded the critical thickness. For the $GaAs_{0.965}N_{0.035}$ epilayer the critical thickness was found to be between 50 and 80 nm. The values obtained for the critical thickness are about two times larger than the theoretical prediction [86]. Also Uesugi *et al* [86] found that the critical thickness for $GaAs_{1-x}N_x$ on GaAs is larger than predicted by the theory. They were able to grow coherent epilayers having a thickness of up to six times the theoretical critical thickness. However, the values obtained by us show that the real critical thickness is smaller than the one obtained from the relaxation state of the layer by HRXRD.

5.2. Point defects

Several kinds of point defect have been reported to exist in arsenide–nitrides. The degradation of the photoluminescence intensity [39, 49] and the carrier transport properties [87, 88] with increasing N composition indicate an increasing concentration of non-radiative recombination centres and carrier traps. The formation of the defects is specific to the growth conditions and thus the consistent identification of these defects has been difficult. However, the following point defects are identified in arsenide–nitrides: As_{Ga} antisites, N interstitials, Ga vacancies, and impurities like oxygen, carbon and hydrogen. As_{Ga} antisites were found from MBE-grown material in the optically detected magnetic resonance studies and their density was found to decrease during annealing [89, 90]. N interstitials were found in MBE-grown material by an ion-channelling technique and their concentration also decreased during annealing [91, 92]. Zhang and Wei [93] showed with thermodynamic calculations that the N–N split interstitial has relatively low formation energy and that it forms a midgap electron state. The impurities are found mainly from MOVPE-grown materials. Oxygen was found to form a midgap non-radiative recombination centre [94]. Carbon is known to act as a p-type dopant, and the incorporation of carbon is enhanced in arsenide–nitrides [36, 44]. Hydrogen is found in MOVPE-grown materials in large quantities and the high concentration of hydrogen was also found to remain after annealing [44]. Thus, hydrogen is strongly bonded to the lattice. However, the role of hydrogen on the material properties is not clear. Hydrogen was found to passivate nitrogen in MBE-grown arsenide–nitrides hydrogenated after growth [95, 96]. The effect disappeared after annealing, which means that hydrogen is in a different configuration in MOVPE-grown arsenide–nitrides.

Ga vacancies were found in MBE-grown material [92], and also in our MOVPE-grown GaAsN epilayers [97]. The vacancies in our samples grown at $>500\,^{\circ}C$ probably belong to defect complexes with some other defects such as As_{Ga} or N_{Ga} antisites, because isolated Ga vacancies are not stable at temperatures above $300\,^{\circ}C$ [98]. Figure 6 shows the experimental gallium vacancy concentration and the low-temperature PL intensity of our GaAsN samples before and after annealing. The vacancy concentration increases with the N concentration up to the order of 10^{18} cm^{-3} and anticorrelates with the PL intensity. Annealing at $700\,^{\circ}C$ for 10 min under H_2 carrier gas flow and TBAs excess ambient reduces the vacancy concentration by a factor of five compared to that found in as-grown material. The anticorrelation of the gallium vacancy concentration and the PL intensity suggests that the defect complexes containing gallium vacancies may act as non-radiative recombination centres in GaAsN. Since the decrease of the PL intensity with increasing N concentration is very drastic, other non-radiative mechanisms are most likely present and contribute to the decrease of the PL intensity.

6. GaInNAs quantum dot structures

Besides using dilute nitrides as gain media, the emission wavelength can be pushed beyond the limit of 1.2 μm of GaAs-based structures by using coherently strained self-organized

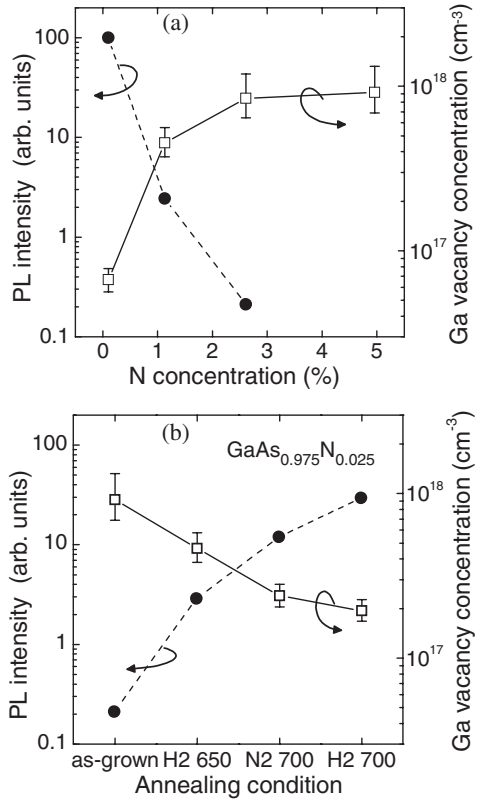

Figure 6. Gallium vacancy concentration and PL intensity of 170 nm-thick GaAsN epilayers as a function of (a) N concentration and (b) annealing condition. The lines are guides to the eye.

three-dimensional In(Ga)As islands as quantum dots (QDs). The emission wavelength can be largely tuned by QD size and composition on a given substrate. QD lasers operating in the 1.3 μm spectral range have been realized [99–102] and very recently an InAs/InGaAs high performance QD laser operating at 1.51 μm was demonstrated [103]. The QD lasers are expected to have several advantages such as decreased transparency current, increased material gain, large characteristic temperature, decreased chirp and increased differential gain. Indeed, low threshold current densities ($<$7 A cm^{-2}/ QD sheet), low internal losses ($\sim$1–3 cm^{-1}) and high quantum efficiencies ($>$80–96%) have been achieved simultaneously [102]. Therefore, it would be interesting to combine the dilute-nitride and QD technologies. Recently, Sopanen *et al* [104] proposed and demonstrated the use of self-assembled GaInNAs QDs to achieve 1.55 μm room-temperature emission on GaAs. In this section we present a review on the current research of GaInNAs QDs with the focus on our MOVPE-grown structures.

6.1. Growth of self-organized GaInNAs QDs

The technique of QD fabrication employs self-organized growth of uniform nanometre-scale three-dimensional islands in the Stranski–Krastanow growth mode [105]. Good size and shape uniformity of islands can be realized in appropriate growth conditions. The islands can also be stacked by growing a thin layer between the QD sheets, resulting in three-dimensionally ordered arrays of QDs. The first GaInNAs QDs reported were grown by gas-source MBE [104]. In that study PL wavelengths of up to 1.52 μm were detected at room temperature from a single layer of $Ga_{0.3}In_{0.7}N_{0.04}As_{0.96}$ QDs. Since then MOVPE [106], solid-source MBE [107, 108] and chemical beam epitaxy (CBE) [109–111] have been used to grow these quaternary QDs.

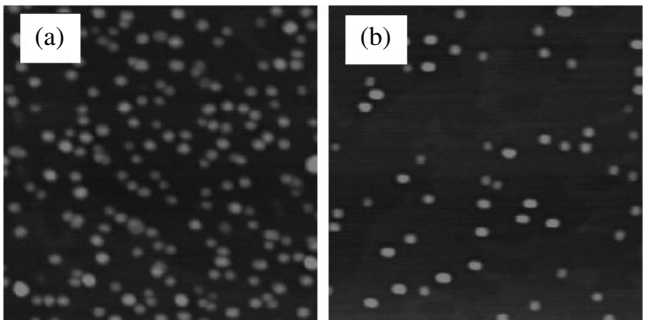

Figure 7. AFM images taken from QD samples grown at 530 °C with (a) 4.5 ML $Ga_{0.4}In_{0.6}NAs$ and (b) 4.5 ML $Ga_{0.4}In_{0.6}As$. The scan size is $0.5 \times 0.5\ \mu m^2$.

Figure 7(a) shows an AFM image from a 4.5 ML $Ga_{0.4}In_{0.6}NAs$ QD sample. The areal density and the average height of the islands are $5 \times 10^{10}\,cm^{-2}$ and 5 nm, respectively. An AFM image from a reference $Ga_{0.4}In_{0.6}As$ sample grown without DMHy flow is shown in figure 7(b). The island density in this N-free sample is smaller ($2 \times 10^{10}\ cm^{-2}$) and the islands are higher on average (8 nm) compared to the sample grown with DMHy flow. This is in contrast to the results that were observed for MBE growth [90]. However, a similar tendency was observed for CBE-grown GaInNAs QDs with N composition of up to 1% [110]. The reason for the larger dot density and smaller size of GaInNAs QDs could be related to the migration length of adatoms. The nitrogen atom may change the surface potential due to its strong bond and decrease the migration length on the surface [110]. PL studies of the overgrown QD samples showed that the PL peak of the $Ga_{0.4}In_{0.6}As$ reference sample was actually at smaller energies compared to the sample grown with DMHy flow. This indicates that a negligible amount of nitrogen was incorporated into the islands. The energy difference can be explained by the larger average height of the $Ga_{0.4}In_{0.6}As$ islands. As discussed before, the N incorporation has a strong dependence on In composition in the MOVPE growth, which explains the lack of nitrogen in the dots having a large indium content.

We tried to improve the N incorporation by using less indium in the dots. Figure 8 shows the dependence of the island density and the average island height on the DMHy/TBAs ratio for $Ga_{0.55}In_{0.45}NAs$ QD samples with a coverage of 8 ML. The island densities in the $Ga_{0.55}In_{0.4}NAs$ QD samples are significantly larger compared to the $Ga_{0.55}In_{0.45}As$ reference sample for all the used DMHy/TBAs ratios. Thus, by using DMHy during the island growth the island density can be increased by one order of magnitude. On the other hand, the island size can be varied to some extent by changing the DMHy/TBAs ratio. Unfortunately, PL studies of overgrown islands indicated that the N incorporation was still negligible, as can be seen in figure 9. However, an enhancement of the 1.3 μm room-temperature luminescence by a factor of about three was observed in the $Ga_{0.55}In_{0.45}NAs$ QD samples grown with DMHy flow. We propose that the DMHy flow can be used as an additional parameter in the MOVPE growth to alter the size and areal density of the GaInAs QDs. Also the optical properties of the QDs can be improved by using DMHy during the island growth.

Results obtained by other groups with different growth methods show red-shift of the QD PL emission wavelength, indicating successful incorporation of nitrogen into the QDs. However, the PL intensity of the QDs decreases and the PL peak broadens very fast with increasing N composition, regardless of the growth method. Very recently, Makino *et al* [112] investigated thermal annealing of GaInNAs QDs. In addition to the increase in the PL intensity, they observed a larger blue-shift of the PL peak wavelength compared to a GaInNAs QW and

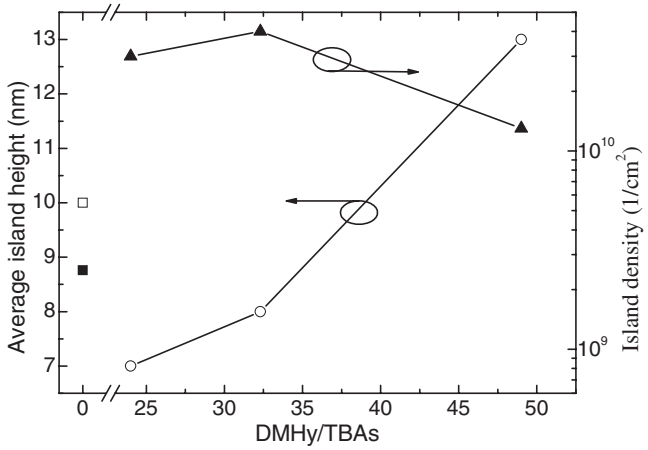

Figure 8. Average island height and island density as a function of DMHy/TBAs ratio for nominally 8 ML-thick $Ga_{0.55}In_{0.45}NAs$ QD samples. The squares show the respective data for the reference $Ga_{0.55}In_{0.45}As$ QD sample.

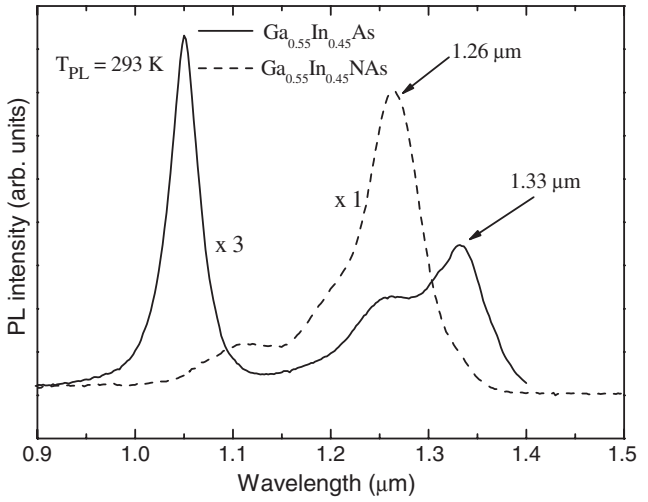

Figure 9. Room-temperature PL spectra from 8 ML $Ga_{0.55}In_{0.45}NAs$ and $Ga_{0.55}In_{0.45}As$ QD samples grown at 520 °C. The reference sample exhibits a dominating wetting layer transition at 1.05 μm. The $Ga_{0.55}In_{0.45}NAs$ sample shows a well pronounced ground state transition at 1.26 μm and no wetting layer transition, indicating efficient capture of the carriers into the QDs. The integrated PL intensity of the $Ga_{0.55}In_{0.45}NAs$ sample is about three times larger than that of the reference sample.

suggested that the In–Ga interdiffusion was enhanced in the QD system. The first (and the only one known to us) GaInNAs QD laser was also realized by Makino *et al* [110]. The device had an edge-emitting geometry and operated under pulsed condition at 1.02 μm. The threshold current density of this device (1.9 kA cm^{-2}) was about ten times higher than in In(Ga)As QD lasers. To conclude this section, we point out that GaInNAs QDs have not been under very wide research interest so far, and a lot of research work is needed to improve the homogeneity and optical quality of the material.

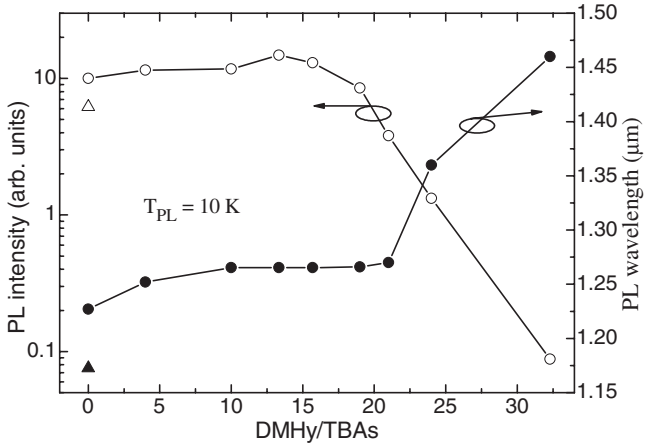

Figure 10. Dependence of the PL intensity and wavelength of the $In_{0.5}Ga_{0.5}As/Ga_{0.85}In_{0.15}NAs$ QDs on the DMHy/TBAs ratio used in the growth of the barrier layer. The triangles show the respective data for QDs embedded in GaAs.

6.2. In(Ga)As/GaInNAs QD structures

The self-organized growth of In(Ga)As QDs provides only limited control of the interrelated size and density of the islands, making it difficult to reach the technologically important 1.3 μm region. A variety of techniques have been proposed to fabricate QDs emitting at longer wavelengths: (1) alternating deposition [113, 114], (2) strain reducing barrier layers [115, 116], (3) activated alloy phase separation [117], and (4) very low growth rates (<0.01 ML s^{-1}) to increase the sizes of the QDs [118]. The most widely used and successful methods have been to use InGaAs or InAlAs strain reducing layers or activated alloy phase separation. There are several reports of these techniques showing the tunability of the light emission in the 1.3–1.55 μm wavelength range [113–116, 119–122]. Recently, it was proposed that GaInNAs could be used as a barrier material for InAs QDs [123]. More recently, room-temperature PL at 1.55 μm with intensity comparable to that of the GaInNAs/GaAs QWs emitting at 1.3 μm was demonstrated from MBE-grown InAs/GaInNAs QD structures [124]. It was shown that in addition to the band gap decrease of the layer covering the QDs, the red-shift of the PL emission could be due to the increase of the QD sizes. Application of tensile-strained GaAsN capping layers to InAs QDs was also proposed [125], which led to improved homogeneity and luminescence efficiency of the InAs QDs and extended emission wavelength of up to 1.55 μm.

Since we found the nitrogen incorporation with MOVPE into GaInNAs QDs to be very difficult, we decided to use GaInNAs as a barrier material for $In_{0.5}Ga_{0.5}As$ QDs. InGaAs was chosen as the QD material instead of InAs since MOVPE-grown InAs easily forms large dislocated clusters. By using a nitrogen-free 5 nm-thick $In_{0.2}Ga_{0.8}As$ layer grown on top of the QDs, we were able to shift the room-temperature PL wavelength from 1.27 to 1.42 μm [126]. At the same time the PL intensity was increased by a factor of three compared to the conventional GaAs cover. The strain in the QDs was partly reduced due to the relaxation of the lattice constraint in the growth direction. This, together with the decrease of the in-plane potential barrier height, led to the increase in the PL wavelength. Figure 10 shows the development of the low-temperature QD PL wavelength and intensity as a function of the DMHy/TBAs ratio when a 10 nm-thick $Ga_{0.85}In_{0.15}N_xAs_{1-x}$ ($0 \leqslant x \leqslant 0.035$) layer was used on top of the QDs. As nitrogen was introduced into the barrier, the PL peak red-shifted first further, but then

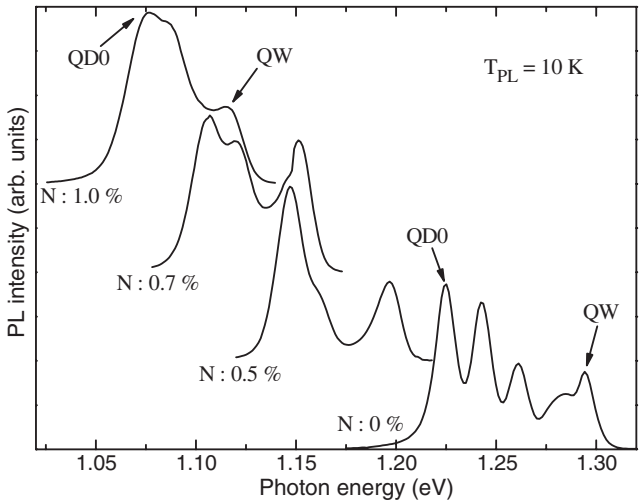

Figure 11. Low-temperature PL spectra of the strain-induced $Ga_{0.8}In_{0.2}N_xAs_{1-x}$ QD samples with $0 \leqslant x \leqslant 0.01$. Quantum well (QW) and quantum dot ground-state (QD0) peaks have been marked.

remained at the same wavelength up to a DMHy/TBAs ratio of 19. The PL intensity increased slightly and stayed higher than that obtained with the GaAs cover until the DMHy/TBAs ratio was increased above 20. Further increase in the DMHy/TBAs ratio resulted in type-II band alignment, seen as a drastic decrease of the PL intensity and a sudden redshift of the PL peak. Temperature dependent PL measurements indicated an increasingly rapid decay of the PL intensity with increasing N composition and no room-temperature luminescence was detected from samples grown with DMHy/TBAs ratios larger than 21. We conclude that by using a nitrogen-containing layer on top of the $In_{0.5}Ga_{0.5}As$ QDs, a slight increase in the PL wavelength and intensity was observed in the 1.3 μm wavelength range. However, it seems more beneficial to use InAs/GaInNAs QD structures since the small band gap of InAs (0.4 eV) allows for larger tunability of the QD emission wavelength. The latest results suggest that the InAs/GaInNAs QD system has potential characteristics for the fabrication of 1.3 and 1.55 μm light emitting devices on GaAs substrates [124].

6.3. Strain-induced GaInNAs/GaAs QDs

The use of self-organized islands as stressors was first demonstrated by Sopanen *et al* [127]. More recently, we have fabricated strain-induced GaInNAs QDs by using self-organized InP stressor islands grown on top of a $Ga_{0.8}In_{0.2}N_xAs_{1-x}$ ($0 \leqslant x \leqslant 0.013$) QW [128]. The InP islands act as stressors inducing a lateral parabolic QD potential in the QW due to tensile strain. This lateral potential together with the vertical QW confinement add up to a three-dimensional confinement potential. Therefore, a QD is formed into the QW under the InP island. The base diameter, the height and the island density of the InP islands were measured by AFM to be about 100 nm, 20 nm and 1–2 $\times$ 10^9 cm^{-2}, respectively.

Low-temperature PL studies of the samples with increasing N concentration showed that the PL peaks of the samples containing nitrogen were broader and fewer excited states, typically only one, were seen compared to the nitrogen-free sample (figure 11). A redshift of about 200 meV for the QW and QD peaks was observed as the N composition was increased from 0 to 1%. Figure 12 shows the full width at half maximum (FWHM) of the QW and QD ground

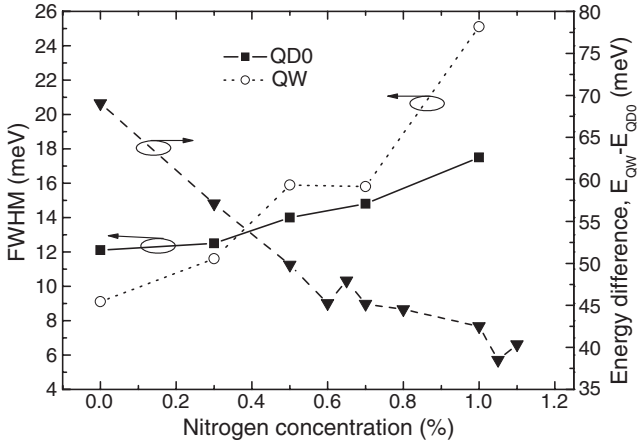

Figure 12. FWHM of the low-temperature (10 K) QW and QD0 PL peaks as a function of the N concentration of the QW. The energy difference of the PL peaks is also shown.

state (QD0) PL peaks as a function of the N concentration. The energy separation between the QW and QD0 peaks is also shown. The FWHM of the QW peak increased from 9 to 25 meV when the N concentration was increased from 0 to 1%. Since the recombination linewidth of a single QD is very narrow, the broadening is probably due to composition or thickness variations in the QWs containing nitrogen. However, the FWHM of the QD0 peak was not as strongly affected by nitrogen. The lateral variation in the composition or thickness may take place in the scale of less than the diameter of the QDs (about 50 nm), because the QD peaks would otherwise broaden similarly to the QW peak. The energy difference of the PL peaks decreased from 69 meV for the nitrogen-free sample to about 40 meV for N composition of about 1%. Carrier localization into states located few tens of millielectronvolt below the band edge of the QW [129, 130] could explain such a decrease in the energy difference. The carrier localization can be explained by the potential minima originated from the composition and thickness fluctuations in the QW. Further proof for the carrier localization was obtained from time-resolved PL measurements [128].

7. Conclusion

GaInNAs/GaAs QW and QD structures and GaAsN epilayers were grown by MOVPE. The MOVPE growth parameters were discussed and compared to the results with MBE. Post-growth thermal annealing and laser irradiation were found to have different effects on the PL properties of GaInNAs QWs; with laser treatment no blue-shift of the PL peak was observed. GaAsN epilayers were shown to contain Ga vacancies in defect complexes. The vacancy concentration was found to anticorrelate with the PL intensity, thus suggesting that the defect complexes may act as non-radiative recombination centres in GaAsN. The critical thickness for misfit dislocation formation of GaAsN on GaAs was studied by synchrotron x-ray topography and found to be about twice as large as the theoretical prediction. The formation and optical properties of self-organized and strain-induced GaInNAs QDs were investigated. Although the N incorporation into GaInNAs QDs was found to be very difficult by MOVPE, the size of the GaInNAs islands could be controlled and their optical properties improved by using DMHy flow during the island growth. GaInNAs was also used as a barrier layer for $In_{0.5}Ga_{0.5}As$

QDs and an increase in the PL wavelength and intensity in the 1.3 μm wavelength range was observed.

References

[1] Kondow M, Uomi K, Niwa A, Watahiki S and Yazawa Y 1996 *Japan. J. Appl. Phys.* **35** 1273
[2] Ramakrishnan A, Steinle G, Supper D, Degen C and Ebbinghaus G 2002 *Electron. Lett.* **38** 322
[3] Vukusic J *et al* 2003 *Electron. Lett.* **39** 662
[4] Murray C, Newman F, Sun S, Clevenger J, Bossert D, Wang C, Hou H and Stail R 2002 *SPIE Proc.* **4649** 31
[5] Kovsh A R, Wang J S, Hsiao R S, Chen L P, Livshits D A, Lin G, Ustinov V M and Chi J Y 2003 *Electron. Lett.* **39** 1726
[6] Gollub D, Fischer M, Kamp M and Forchel A 2002 *Appl. Phys. Lett.* **81** 4330
[7] Gollub D, Moses S, Fischer M and Forchel A 2003 *Electron. Lett.* **39** 777
[8] Gollub D, Moses S, Kamp M and Forchel A 2003 *Electron. Lett.* **39** 1815
[9] Okhotnikov O G, Jouhti T, Konttinen J, Karirinne S and Pessa M 2003 *Opt. Lett.* **28** 364
[10] Weyers M, Sato M and Ando H 1992 *Japan. J. Appl. Phys.* **31** L853
[11] Pozina G, Ivanov I, Monemar B, Thordson J V and Andersson T G 1998 *J. Appl. Phys.* **84** 3830
[12] Bi W G and Tu C W 1997 *Appl. Phys. Lett.* **70** 1609
[13] Kondow M, Uomi K, Hosomi K and Mozume T 1994 *Japan. J. Appl. Phys.* **33** L1056
[14] Perkins J D, Mascarenhas A, Zhang Y, Geisz J F, Friedman D J, Olson J M and Kurtz S R 1999 *Phys. Rev. Lett.* **82** 3312
[15] Klar P J, Grüning H, Heimbrodt W, Koch J, Höhnsdorf F, Stolz W, Vicente P M A and Camassel J 2000 *Appl. Phys. Lett.* **76** 3439
[16] Skierbiszewski C *et al* 2000 *Appl. Phys. Lett.* **76** 2409
[17] Hai P N, Chen W M, Buyanova I A, Xin H P and Tu C W 2000 *Appl. Phys. Lett.* **77** 1843
[18] Pan Z, Li L H, Lin Y W, Sun B Q, Jiang D S and Ge W K 2001 *Appl. Phys. Lett.* **78** 2217
[19] Perlin P, Subramanya S G, Mars D E, Kruger J, Shapiro N A, Siegle H and Weber E R 1998 *Appl. Phys. Lett.* **73** 3703
[20] Shan W, Walukiewicz W, Ager J W III, Haller E E, Geisz J F, Friedman D J, Olson J M and Kurtz S R 1999 *Phys. Rev. Lett.* **82** 1221
[21] Perkins J D, Mascarenhas A, Geisz J F and Friedman D J 2001 *Phys. Rev.* B **64** 121301(R)
[22] Shan W, Walukiewicz W, Ager J W III, Haller E E, Geisz J F, Friedman D J, Olson J M and Kurtz S R 1999 *Appl. Phys. Lett.* **86** 2349
[23] Wu J, Shan W and Walukiewicz W 2002 *Semicond. Sci. Technol.* **17** 860
[24] Kent P R C and Zunger A 2001 *Phys. Rev. Lett.* **86** 2609
[25] Kent P R C and Zunger A 2001 *Phys. Rev.* B **64** 115208
[26] Kent P R C and Zunger A 2001 *Appl. Phys. Lett.* **79** 2339
[27] Kent P R C, Bellaiche L and Zunger A 2002 *Semicond. Sci. Technol.* **17** 851
[28] O'Reilly E P, Lindsay A, Tomic S and Kamal-Saadi M 2002 *Semicond. Sci. Technol.* **17** 870
[29] O'Reilly E P and Lindsay A 1999 *Phys. Status Solidi* b **216** 131
[30] Kurtz S V, Modine N A, Jones E D, Allerman A A and Klem J 2002 *Semicond. Sci. Technol.* **17** 843
[31] Harris J S Jr 2002 *Semicond. Sci. Technol.* **17** 880
[32] Skierbiszewski C 2002 *Semicond. Sci. Technol.* **17** 803
[33] Riechert H, Ramakrishnan A and Steinle G 2002 *Semicond. Sci. Technol.* **17** 892
[34] Schlenker D, Miyamoto T, Pan Z, Koyama F and Iga K 1999 *J. Cryst. Growth* **196** 67
[35] Kurtz S, Reedy R, Barber G D, Geisz J F, Friedman D J, McMahon W E and Olson J M 2002 *J. Cryst. Growth* **234** 318
[36] Kurtz S, Reedy R, Keyes B, Barber G D, Geisz J F, Friedman D J, McMahon W E and Olson J M 2002 *J. Cryst. Growth* **234** 323
[37] Wei X, Wang G H, Zhang G Z, Zhu X P, Ma X Y and Chen L H 2002 *J. Cryst. Growth* **236** 516
[38] Lum R M and Klingert J K 1989 *J. Appl. Phys.* **66** 3820
[39] Toivonen J, Hakkarainen T, Sopanen M and Lipsanen H 2000 *J. Cryst. Growth* **221** 456
[40] Uesugi K and Suemune I 1998 *J. Cryst. Growth* **189/190** 490
[41] Ptak A J, Kurtz S, Curtis C, Reedy R and Olson J M 2002 *J. Cryst. Growth* **243** 231
[42] Pohl U W, Möller C, Knorr K, Richter W, Gottfriedsen J, Schumann H, Rademann K and Fielicke A 1999 *Mater. Sci. Eng.* B **59** 20
[43] Odnoblyudov V A, Egorov A Y, Kovsh A R, Zhukov A E, Maleev N A, Semenova E S and Ustinov V M 2001 *Semicond. Sci. Technol.* **16** 831

[44] Moto A, Takahashi M and Takagishi S 2000 *J. Cryst. Growth* **221** 485
[45] Ougazzaden A, Bellego Y L, Rao E V K, Juhel M, Leprince L and Patriache G 1997 *Appl. Phys. Lett.* **70** 2861
[46] Plaine G-Y, Asplund C, Sundgren P, Mogg S and Hammar M 2002 *Japan. J. Appl. Phys.* **41** 1040
[47] Bhat R, Caneau C, Salamanca-Riba L, Bi W and Tu C W 1998 *J. Cryst. Growth* **195** 427
[48] Friedman D J, Geisz J F, Kurtz S R and Olson J M 1998 *J. Cryst. Growth* **195** 409
[49] Hakkarainen T, Toivonen J, Sopanen M and Lipsanen H 2002 *J. Cryst. Growth* **234** 631
[50] Harmand J C, Ungaro G, Largeau L and Le Roux G 2000 *Appl. Phys. Lett.* **77** 2482
[51] Egorov A Y *et al* 2001 *J. Cryst. Growth* **227/228** 545
[52] Kondow M and Kitatani T 2002 *Semicond. Sci. Technol.* **17** 746
[53] Buyanova I A, Chen W M, Pozina G, Berman J P, Monemar B, Xin H P and Tu C W 1999 *Appl. Phys. Lett.* **75** 501
[54] Polimeni A, Capizzi M, Geddo M, Fischer M, Reinhardt M and Forchel A 2001 *Phys. Rev.* B **63** 195320
[55] Li W, Jouhti T, Peng C S, Konttinen J, Laukkanen P, Pavelescu E-M, Dumitrescu M and Pessa M 2001 *Appl. Phys. Lett.* **79** 3386
[56] Riechert H, Egorov A Y, Livshits D, Borchert B and Illek S 2000 *Nanotechnology* **11** 201
[57] Tansu N, Kirsch N and Mawst L J 2002 *Appl. Phys. Lett.* **81** 2523
[58] Tansu N and Mawst L J 2002 *IEEE Photon. Technol. Lett.* **14** 444
[59] Tansu N, Yeh J Y and Mawst L J 2003 *Appl. Phys. Lett.* **83** 2512
[60] Buyanova I A, Chen W M, Pozina G, Hai P N, Monemar B, Xin H P and Tu C W 2001 *Mater. Sci. Eng.* B **82** 143
[61] Kaschner A, Lüttgert T, Born H, Hoffmann A, Egorov A Y and Riechert H 2001 *Appl. Phys. Lett.* **78** 1391
[62] Spruytte S G, Coldren C W, Harris J S, Wampler W, Krispin P, Ploog K and Larson M C 2001 *J. Appl. Phys.* **89** 2314
[63] Kaplar R J, Arehart R, Ringel S A, Allerman A A, Sieg R M and Kurtz S R 2001 *J. Appl. Phys.* **90** 3405
[64] Krispin P, Spruytte S G, Harris J S and Ploog K H 2001 *J. Appl. Phys.* **89** 6294
[65] Spruyette A G, Larson M C, Wampler W, Coldren C W, Petersen H E and Harris J S 2001 *J. Cryst. Growth* **227/228** 506
[66] Peng C S, Pavelescu E-M, Jouhti T, Konttinen J, Fodchuk I M, Kyslovsky Y and Pessa M 2002 *Appl. Phys. Lett.* **80** 4720
[67] Grillo V, Albrecht M, Remmele T, Strunk H, Egorov A Y and Riechert H 2001 *J. Appl. Phys.* **90** 3792
[68] Kim K and Zunger A 2001 *Phys. Rev. Lett.* **12** 2609
[69] Klar P J, Grünning H, Koch J, Schäfer S, Volz K, Stolz W, Heimbrodt W, Saadi A M, Lindsay A and O'Reilly E P 2001 *Phys. Rev.* B **64** 121203
[70] Gambin V, Lordi V, Ha W, Wistey M, Takizawa T, Uno K, Friedrich S and Harris J 2003 *J. Cryst. Growth* **251** 408
[71] Jouhti T, Peng C S, Pavelescu E-M, Konttinen J, Gomes L A, Okhotnikov O G and Pessa M 2002 *IEEE J. Sel. Top. Quantum Electron.* **8** 787
[72] Yang X, Heroux J B, Mei L F and Wang W I 2001 *Appl. Phys. Lett.* **78** 4068
[73] Ha W, Gambin V, Vistey M, Bank S, Yuen H, Kim S and Harris J S 2002 *Electron. Lett.* **38** 277
[74] Ha W, Gambin V, Vistey M, Bank S, Yuen H, Kim S and Harris J S 2002 *IEEE Photon. Technol. Lett.* **14** 591
[75] Li L H, Sallet V, Patriarche G, Largeau L, Bouchhoule S, Merghem K, Travers L and Harmand J C 2003 *Electron. Lett.* **39** 519
[76] Wistey M A, Bank S R, Yuen H B, Goddard L L and Harris J S 2003 *Electron. Lett.* **39** 1822
[77] Ha W, Gambin V, Bank S, Wistey M, Yuen H, Kim S and Harris J S 2002 *IEEE J. Quantum Electron.* **38** 1260
[78] Rao E V K, Ougazzaden A, Bellego Y and Juhel M 1998 *Appl. Phys. Lett.* **72** 1409
[79] Toivonen J, Hakkarainen T, Sopanen M and Lipsanen H 2003 *IEE Proc. Optoelectron.* **150** 68
[80] Shonozuka Y 2001 *Physica* B **308–310** 506
[81] Höhnsdorf F, Koch J, Agert C and Stolz W 1998 *J. Cryst. Growth* **195** 391
[82] Suemune I, Uesugi K and Seong T Y 2002 *Semicond. Sci. Technol.* **17** 755
[83] Volovik B V, Kovsh A R, Passenberg W, Kuenzel H, Grote N, Cherkashin N A, Musikhin Y G, Ledentsov N N, Bimberg D and Ustinov V M 2001 *Semicond. Sci. Technol.* **16** 186
[84] Toivonen J, Tuomi T, Riikonen J, Knuuttila L, Hakkarainen T, Sopanen M, Lipsanen H, McNally P J, Chen W and Lowney D 2003 *J. Mater. Sci., Mater. Electron.* **14** 267
[85] Uesugi K, Morooka N and Suemune I 1999 *Appl. Phys. Lett.* **74** 1254
[86] Uesugi K, Morooka N and Suemune I 1999 *J. Cryst. Growth* **201/202** 355
[87] Kurtz S R, Allerman A A, Seager C H, Sieg R M and Jones E D 2000 *Appl. Phys. Lett.* **77** 400
[88] Fleck A, Robinson B J and Thompson D A 2001 *Appl. Phys. Lett.* **78** 1694
[89] Thinh N Q, Buyanova I A, Hai P N, Chen W M, Xin H P and Tu C W 2001 *Phys. Rev.* B **63** 033203

[90] Thinh N Q, Buyanova I A, Chen W M, Xin H P and Tu C W 2001 *Appl. Phys. Lett.* **79** 3089
[91] Ahlgren T, Vainonen-Ahlgren E, Likonen J, Li W and Pessa M 2002 *Appl. Phys. Lett.* **80** 2314
[92] Li W, Pessa M, Ahlgren T and Dekker J 2001 *Appl. Phys. Lett.* **79** 1094
[93] Zhang S B and Wei S-H 2001 *Phys. Rev. Lett.* **86** 1789
[94] Balcioglu A, Ahrenkiel R K and Friedman D J 2000 *Appl. Phys. Lett.* **76** 2397
[95] Baldassarri H v H G, Bissiri M, Polimeni A, Capizzi M, Fischer M, Reinhardt M and Forchel A 2001 *Appl. Phys. Lett.* **78** 3472
[96] Bissiri M *et al* 2002 *Phys. Rev.* B **65** 235210
[97] Toivonen J, Hakkarainen T, Sopanen M, Lipsanen H, Oila J and Saarinen K 2003 *Appl. Phys. Lett.* **82** 40
[98] Corbel C, Pierre F, Saarinen K, Hautojärvi P and Moser P 1992 *Phys. Rev.* B **45** 3386
[99] Huffaker D L, Park G, Zou Z, Shchekin O B and Deppe D G 1998 *Appl. Phys. Lett.* **73** 2564
[100] Park G, Shchekin O B, Csutak S, Huffaker D L and Deppe D G 1999 *Appl. Phys. Lett.* **75** 3267
[101] Kovsh A R *et al* 2002 *Electron. Lett.* **38** 1104
[102] Ledentsov N N 2002 *IEEE J. Sel. Top. Quantum Electron.* **8** 1015 and references therein
[103] Ledentsov N N, Kovsh A R, Zhukov A E, Maleev N A, Mikhrin S S, Vasil'ev A P, Semenova E S, Maximov M V, Shernyakov Y M, Kryszhanovskaya N V, Ustinov V M and Bimberg D 2003 *Electron. Lett.* **39** 1126
[104] Sopanen M, Xin H P and Tu C W 2000 *Appl. Phys. Lett.* **76** 994
[105] Eaglesham D J and Cerullo M 1990 *Phys. Rev. Lett.* **64** 1943
[106] Hakkarainen T, Toivonen J, Sopanen M and Lipsanen H 2001 *Appl. Phys. Lett.* **79** 3932
[107] Sun Z Z, Yoon S F, Yew K C, Loke W K, Wang S Z and Ng T K 2002 *J. Cryst. Growth* **242** 109
[108] Yew K C, Yoon S F, Sun Z Z and Wang S Z 2003 *J. Cryst. Growth* **247** 279
[109] Makino S, Miyamoto T, Kageyama T, Ikenaga Y, Koyama F and Iga K 2002 *Japan. J. Appl. Phys.* **41** 953
[110] Makino S, Miyamoto T, Kageyama T, Nishiyama N, Koyama F and Iga K 2000 *J. Cryst. Growth* **221** 561
[111] Makino S, Miyamoto T, Ohta M, Kageyama T, Ikenaga Y, Koyama F and Iga K 2003 *J. Cryst. Growth* **251** 372
[112] Makino S, Miyamoto T, Ohta M, Matsuura T, Matsui Y and Koyama F 2003 *Int. Conf. on Indium Phosphide and Related Materials (May 2003)* Paper ThP18, p 460
[113] Mukai K, Ohtsuka N, Sugawara M and Yamazaki S 1994 *Japan. J. Appl. Phys.* **33** L1710
[114] Mirin R P, Ibbetson J P, Nishi K, Gossard A C and Bowers J E 1995 *Appl. Phys. Lett.* **67** 3795
[115] Nishi K, Saito H, Sugou S and Lee J-S 1999 *Appl. Phys. Lett.* **74** 1111
[116] Bloch J, Shah J, Hobson W S, Lopata J and Chu S N G 1999 *Appl. Phys. Lett.* **75** 2199
[117] Maximov M V *et al* 2000 *Phys. Rev.* B **62** 16671
[118] da Silva M J, Quivy A A, Martini S, Lamas T E, da Silva E C F and Leite J R 2003 *Appl. Phys. Lett.* **82** 82646
[119] Seravalli L, Minelli M, Frigeri P, Allegri P, Avanzini V and Franchi S 2003 *Appl. Phys. Lett.* **82** 2341
[120] Liu H Y and Hopkinson M 2003 *Appl. Phys. Lett.* **82** 3644
[121] Yeh N-T, Nee T-E, Chyi J-I, Hsu T M and Huang C C 2000 *Appl. Phys. Lett.* **76** 1567
[122] Passaseo A, Maruccio G, De Vittorio M, Rinaldi R, Cingolani R and Lomascolo M 2001 *Appl. Phys. Lett.* **78** 1382
[123] Egorov A Yu, Bedarev D, Bernklau D, Dumitras G and Riechert H 2001 *Phys. Status Solidi* b **224** 839
[124] Ustinov V M, Egorov A Yu, Odnoblyudov V A, Kryzhanovskaya N V, Musikhin Y G, Tsatsul'nikov A F and Alferov Z I 2003 *J. Cryst. Growth* **251** 388
[125] Zhang X Q, Ganapathy S, Suemune I, Kumano H, Uesugi K, Nabetani Y and Matsumoto T 2003 *Appl. Phys. Lett.* **83** 4524
[126] Hakkarainen T, Toivonen J, Sopanen M and Lipsanen H 2003 *J. Cryst. Growth* **248** 339
[127] Sopanen M, Lipsanen H and Ahopelto J 1995 *Appl. Phys. Lett.* **66** 2364
[128] Koskenvaara H, Hakkarainen T, Sopanen M and Lipsanen H 2003 *J. Mater. Sci. Mater. Electron.* **14** 357
[129] Grenouillet L, Bru-Chevallier C, Guillot G, Gilet P, Duvault P, Vannuffel C, Million A and Chenevas-Paule A 2000 *Appl. Phys. Lett.* **76** 2241
[130] Pinault M-A and Tournie E 2001 *Appl. Phys. Lett.* **78** 1562